Brain Pathology ISSN 1015-6305

RESEARCH ARTICLE

Spatial and Cellular Characterization of mTORC1 Activation after Spinal Cord Injury Reveals Biphasic Increase Mainly Attributed to Microglia/Macrophages

Jacob Kjell[1]; Simone Codeluppi[2]; Anna Josephson[1]; Mathew B. Abrams[1]

Departments of [1] Neuroscience and [2] Medical Biochemistry and Biophysics, Karolinska Institutet, Stockholm, Sweden.

Keywords
astrocyte, neuron, neutrophil, oligodendrocyte progenitor cell, proliferation, S6.

Corresponding author:
Jacob Kjell, M.Sc., Department of Neuroscience, Karolinska Institutet, Retziusväg 8, B2:4, Stockholm 171 77, Sweden (E-mail: *jacob.kjell@ki.se*)

Received 18 November 2013
Accepted 17 February 2014
Published Online Article Accepted 27 February 2014

doi:10.1111/bpa.12135

Abstract

Mechanistic target of rapamycin complex 1 (mTORC1) is an intracellular kinase complex that regulates energy homeostasis and transcription. Modulation of mTORC1 has proven beneficial in experimental spinal cord injury, making this molecular target a candidate for therapeutic intervention in spinal cord injury. However, both inactivation and activation of mTORC1 have been reported beneficial for recovery. To obtain a more complete picture of mTORC1 activity, we aimed to characterize the spatiotemporal activation pattern of mTORC1 and identify activation in particular cell types after contusion spinal cord injury in rats. To be able to provide a spatial characterization of mTORC1 activation, we monitored activation of downstream target S6. We found robust mTORC1 activation both at the site of injury and in spinal segments rostral and caudal to the injury. There was constitutive mTORC1 activation in neurons that was biphasically reduced caudally after injury. We found biphasic mTORC1 activation in glial cells, primarily activated microglia/macrophages. Furthermore, we found mTORC1 activation in proliferating cells, suggesting this may be a function affected by mTORC1 modulation. Our results reveal potential windows of opportunity for therapeutic interference with mTORC1 signaling and immune cells as targets for inhibition of mTORC1 in spinal cord injury.

INTRODUCTION

The serine/threonine protein kinase mechanistic target of rapamycin (mTOR) is the catalytic component of mTOR complex 1 (mTORC1), which controls energy homeostasis and impacts cell growth, motility, proliferation, and other transcription-dependent activities (18). mTORC1 is known to play a role in tumor malignancies and has also been shown to play a role in several CNS pathologies, such as Alzheimer's disease, Parkinson's disease, ischemic stroke, and spinal cord injury (4, 33). In experimental spinal cord injury, modulation of mTORC1 activity has been reported to result in decreased astrocyte reactivity, increased axonal sprouting and autophagy, and decreased pain; however, the beneficial effects of mTORC1 modulation have been produced by both inhibition and activation of mTORC1 (2, 7, 19, 34). Because of the discrepancy between the effects of modulation, manner of modulation, and duration of altered mTORC1 activity, this promising therapeutic target is kept from advancing towards possible clinical applications. mTORC1 is also interesting in a translational context, as there is an inhibitor in clinical use for both Kaposi's sarcoma and transplantation (24, 36). Furthermore, reports to date have for the most part focused on modulatory effects on single cell types, making assessment of overall effect of mTORC1 modulation difficult. Determining the cell types involved and the parameters of spatiotemporal mTORC1 activity after spinal cord injury in preclinical models should help determine whether any form of mTORC1 modulation constitutes a potential treatment for spinal cord injury.

Most investigations of mTORC1 activation in experimental spinal cord injury have focused on modulation of neurons and astrocytes, despite reports that mTORC1 impacts immune cell activity (24, 32). Immune cells such as macrophages/microglia and neutrophils play pivotal roles in the pathophysiology of spinal cord injury (30). The inflammatory response removes cell debris and contributes to wound healing; however, it also plays a role in tissue degeneration, which is considered detrimental to functional outcome (12, 16, 35). Nevertheless, modulating the inflammatory response by changing cell type polarization, cell number, or degree of activity can instead promote regeneration and reduce pathology, thus improving functional outcome (1, 14, 28, 31). The immune response therefore stands out as a central component in recovery from spinal cord injury, but it has not been the focus of previous studies of mTORC1 dynamics in experimental spinal cord injury.

To provide a more complete picture of spontaneous mTORC1 activity, we characterized the spatiotemporal activation of mTORC1 in different cell populations after experimental contusion injury to the spinal cord. Following a moderate contusion injury, we assessed mTORC1 activation by quantifying the immunoreactivity of phosphorylated S6, a downstream target of mTORC1 commonly used as a readout for its activity (27, 37, 39). S6 phosphorylation was assessed in immune cells, neural progenitor cells, and proliferating cells, as well as neurons and astrocytes from 1 to 119 days post-injury.

MATERIALS AND METHODS

Spinal cord injury

Female Sprague Dawley rats (220–230 g; $n = 40$; Scanbur, Stockholm, Sweden) were anesthetized using 2% isoflurane. A laminectomy was performed at thoracic vertebra 10 and the caudal half of vertebra 9 to expose the dorsal surface of the spinal cord. A 10-g weight was then dropped from 25 mm onto the dorsal surface of the exposed spinal cord to induce a moderate contusion injury using a dedicated instrument (Impactor, Keck Center for Neuroscience, Piscataway, NJ, USA) as previously described (13, 17). Postoperatively, animals were treated with antibiotics (0.6 mg/kg trimethoprim; Borgal, Hoechst AG, Friesoythe, Germany) for 7 days and analgesic (0.03 mg/kg buprenorphine; Temgesic, RB Pharmaceuticals Limited, Berkshire, UK) for 3 days. Bladders were manually emptied twice daily for the first 7 days, then once daily until bladder function was regained. Animals were housed three to a cage with a 12-h light/dark cycle and a room temperature of 24–26°C. Food and water were provided *ad libitum*. All experiments were performed according to the Declaration of Helsinki and were approved by the Northern Stockholm Ethical Committee.

Spinal cord preparation

Deeply anesthetized animals (40 mg/kg pentobarbital, i.p.; Nembutal, Apotektet, Stockholm, Sweden) were perfused with 50 ml calcium-free Tyrode's solution containing 0.1 ml heparin (5000 IE/ml) followed by 250 ml formalin/picric acid mixture (4% paraformaldehyde, 0.4% picric acid in 0.1 M phosphate buffer, pH 7.4) via the ascending aorta ($n = 5$ per time point). Spinal cords were dissected and postfixed for 1 h in the same fixative. The tissues were next transferred to 10% sucrose in 0.1 M phosphate-buffered saline, which was changed once per 4 days. Spinal cords were divided into five 7-mm segments, spanning 14 mm caudal and rostral to the injury site (also a 7 mm segment). Segments were embedded in OCT medium and frozen on dry ice, sectioned in a cryostat (Microm HM 500M; GMI, Ramsey, MN, USA), and mounted on gelatin-coated slides.

Immunohistochemistry

A phosphorylated S6 (pS6)-specific antibody (S235/236, Cell Signaling, Danvers, MA, USA) was used to monitor mTORC1 activation. Antibodies for neuronal nuclei (NeuN; Chemicon, Billerica, MA, USA), glial fibrillary acidic protein (GFAP; Dako), neuron-glial antigen 2 (NG2; Millipore, Billerica, MA, USA), OX-42 (Serotec Oxford, UK), ED1 (Serotec Oxford, UK), Ki-67 (BD Pharmingen Oxford, UK), and myeloperoxidase (MPO; Hycult Biotech, Uden, the Netherlands) were used to evaluate neurons, astrocytes, oligodendrocyte progenitors, microglia/macrophages, activated microglia/macrophages, proliferation, and neutrophils, respectively. Primary antibodies were visualized using appropriate secondary antibodies (Cy3 or DyLight™ 488, Jackson Laboratories, Sacramento, CA, USA).

Spinal cord sections (20 µm) mounted on gelatin-coated slides were incubated with primary antibody at 4°C for 24 h. After washing, secondary antibodies were added and sections incubated for 1.5 h at room temperature. Primary and secondary antibodies were diluted in 0.3% Triton-X 100 in 0.1 M PBS. Slides were coated with an anti-fade agent (Prolonged Gold® Invitrogen, Carlsbad, CA, USA) and were visualized using fluorescence microscopy (Nikon Eclipse TE3000, Surrey, UK) if only labeled with one marker or confocal microscopy (Olympus FV1000 CLSM, Hamburg, Germany) if double-labeled.

Image analysis

Cell counts, intensity measurements, and semiquantifications were performed on three sections per spinal segment per animal. From each 7-mm segment, sections from the central 3 mm were used for quantification, and for each time point, five animals were used. NeuN- and pS6-positive neurons were counted on double-labeled sections. pS6 immunoreactivity within the dorsal column was quantified using an appropriate image-processing program (FIJI, available at http://fiji.sc/About). Equal-sized areas placed in the same region were used to measure intensity, with background staining subsequently subtracted.

Statistical analysis

Two-tailed Student's *t*-tests were used for statistical analysis of intensity measures at cystic cavities and number of neurons below the injury. ANOVA with Bonferroni's multiple comparison test was used for statistical analysis of intensity measures at the dorsal column and number of pS6/NeuN-positive cells for all time points. Significance thresholds were determined as $P < 0.05$, $P < 0.01$, and $P < 0.001$. Localizations of pS6 immunoreactivity in different immunohistochemically defined cell types were semiquantified 1 and 42 days after injury, using one, two, or three plus signs to denote proportions of pS6 colocalization.

RESULTS

Biphasic reduction of S6 activation in neurons on injury

In uninjured tissue, constitutive pS6 immunoreactivity was found primarily in neurons of the ventral horns and in neuronal populations of the intermediate zone (Figures 1 and 2A), but not in dorsal horn neurons. After injury, pS6 immunoreactivity remained in the ventral horns caudal and rostral to the site of injury at all investigated time points and remained absent in neurons of the dorsal horns (Supporting Information Figure S1). In the intermediate zone of the gray matter caudal to the injury site, however, we found a biphasic reduction in number of pS6-positive neurons (Figure 2B). The first loss of pS6 immunoreactivity in intermediate-zone neurons was observed at day 1 post-injury, where the mean number of pS6-immunoreactive neurons 7 mm caudal to the injury was 50.3 ± 1.60, compared to 87.2 ± 3.36 in uninjured tissue ($P < 0.001$). This initial loss of pS6 immunoreactivity was followed by a transient increase in number of pS6 immunoreactive neurons, which peaked at 80.8 ± 2.39 on day 21 post-injury and was followed by a period of reduced numbers of pS6-positive neurons compared with uninjured spinal cords at days 42 and 56 post-injury. Seventeen weeks after injury (119 dpi), the number of pS6-immunoreactive neurons remained significantly reduced in the injured spinal cord compared with intact spinal cord (70.2 ± 2.44 and 87.2 ± 3.36,

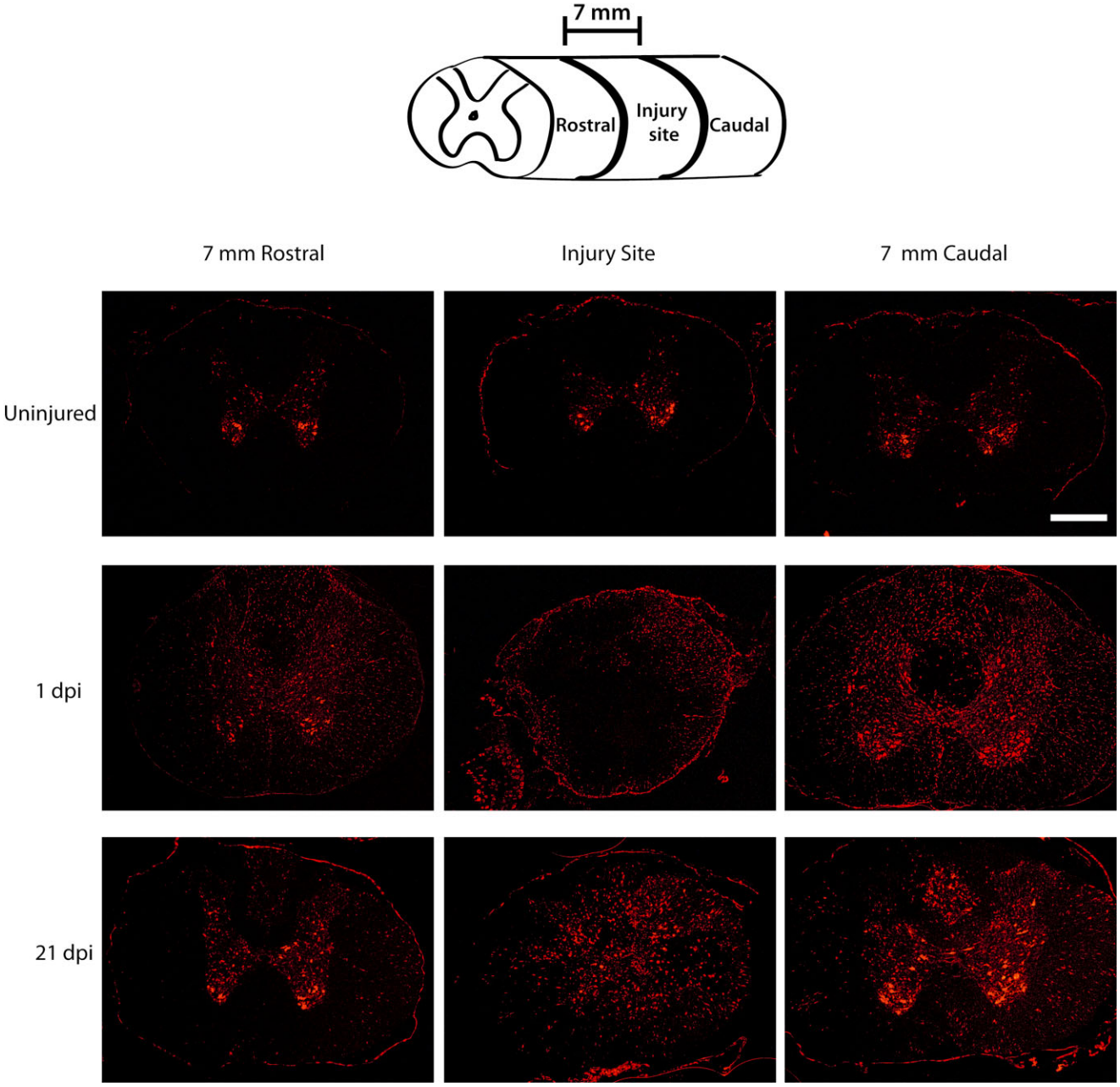

Figure 1. *S6 phosphorylation in the intact and injured spinal cord.* pS6 immunoreactivity in uninjured tissue sections compared to 1 and 21 days post-injury (dpi). The spinal cord illustration defines segments from which the spinal cord sections originate. Sections are taken from the injury site and 7 mm rostral and caudal to the injury site. Scale bar = 250 μm.

respectively; $P < 0.01$). A similar pattern was observed rostral to the injury site, although no significant difference was found compared with uninjured spinal cords 17 weeks after injury (Supporting Information Figure S2).

S6 phosphorylation in glial cells on injury

There was little constitutive pS6 immunoreactivity in white matter of uninjured spinal cords. However, injury induced a robust increase in S6 phosphorylation in many cell populations in the area of white matter tracts of the spinal cord rostral and caudal to the injury site (Figure 1). A biphasic pS6 increase was observed. A first increase of pS6 immunoreactivity seen at day 1 was reduced 7 days after injury to levels comparable with those in uninjured spinal cords. A second increase was observed to start 21 days after injury, this time more focused on specific regions such as the injury site, the cystic cavities, and the rostral dorsal column (Figure 1). This second increase in pS6 immunoreactivity was found to peak at 42 days after

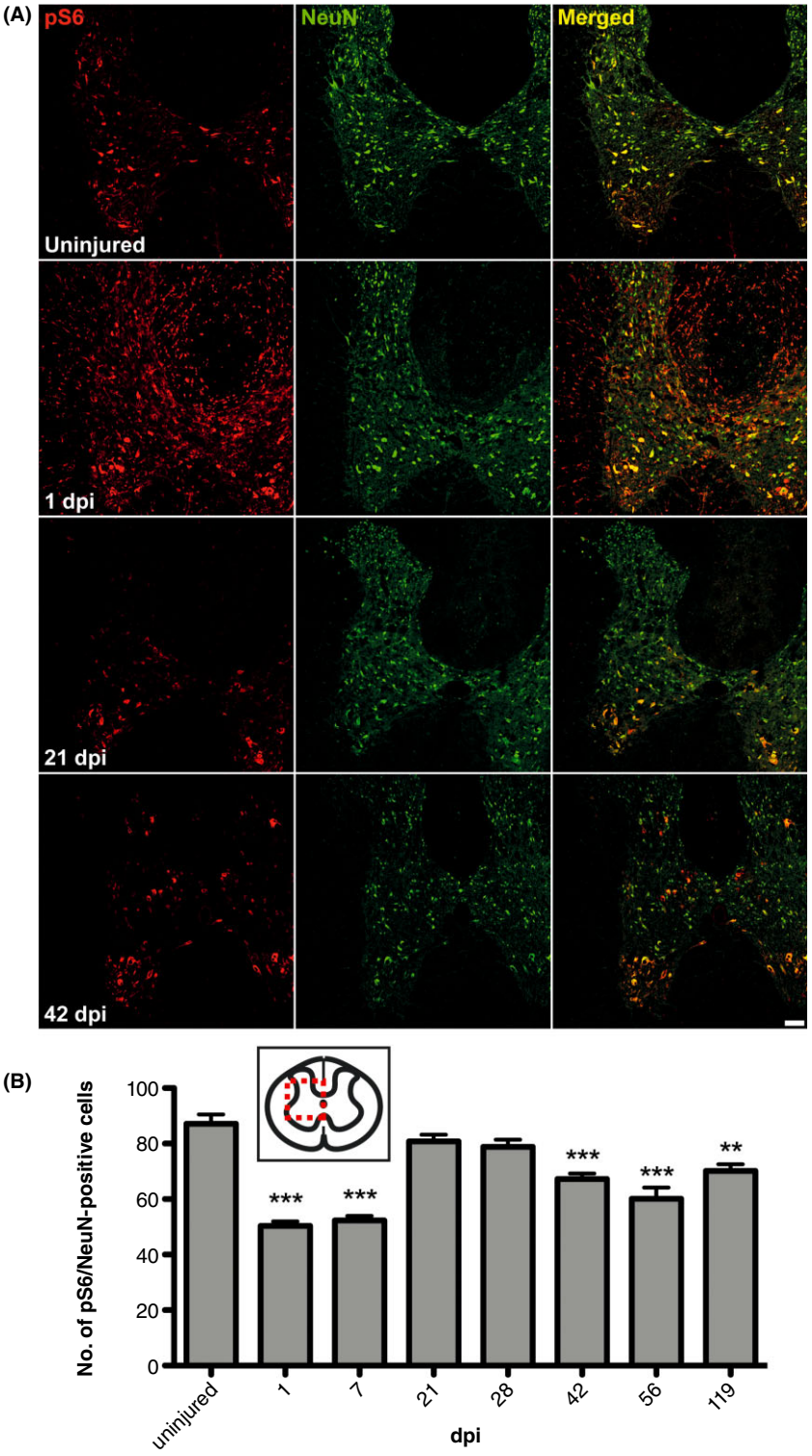

Figure 2. *Biphasic reduction of pS6-positive neurons.* Antibodies to pS6 and NeuN were used to detect S6 activation in neurons 7 mm below the injury site. **A.** Representative pictures showing uninjured tissue and tissue from 1, 21, and 42 days post-injury (dpi). Scale bar = 20 μm. **B.** Quantification of number of pS6- and NeuN-positive cells for all experimental time points. Data presented as mean ± SEM. $^{*}P < 0.05$; $^{**}P < 0.01$; $^{***}P < 0.001$.

injury, followed by a decrease to control levels as observed 119 days after injury. During the biphasic increase of pS6 immunoreactivity, we identified pS6-immunoreactive astrocytes, oligodendrocyte progenitor cells, microglia, and activated microglia/macrophages in the rostral dorsal column and ventrolateral white matter (Figure 3, Supporting Information Figure S3).

First S6 activation in glial cells

The first increase in S6 phosphorylation was found for day 1 after spinal cord injury and had subsided by day 7 after injury. GFAP/pS6-immunoreactive cells were found in white matter, primarily within the dorsal column (Figure 3A, Supporting Information

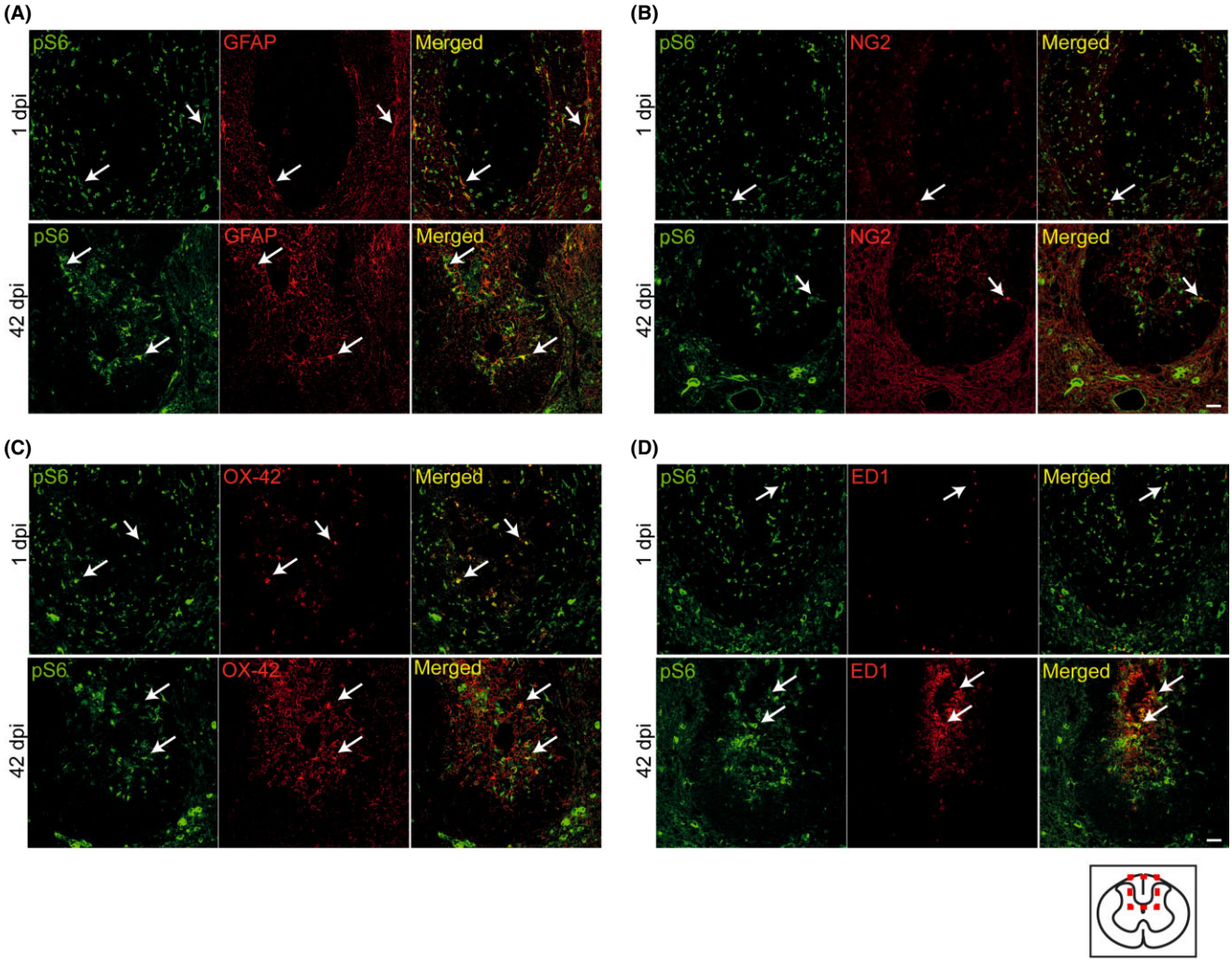

Figure 3. *Types of pS6-positive glial cell types in the dorsal column.* Representative pictures from 7 mm above the injury at the dorsal column 1 and 42 days post-injury, showing colocalization of pS6 with GFAP (**A**), NG2 (**B**), OX42 (**C**), and ED1 (**D**). Scale bar = 20 μm.

Figure S3A). Only a few pS6/NG2-immunoreactive cells were found in the dorsal column; more cells were found in ventrolateral white matter (Figure 3B, Supporting Information Figure S3B). OX-42-immunoreactive cells had diverse morphologies ranging from spiny to round. Many rounded OX-42/pS6-immunoreactive cells were found in the dorsal column, while a higher number of ramified OX-42/pS6-positive cells were found in the ventrolateral white matter (Figure 3C, Supporting Information Figure S3C). ED1/pS6-immunoreactive cells were primarily found in the dorsal column (Figure 3D, Supporting Information Figure S3D).

Second S6 activation in glial cells

The second increase of S6 phosphorylation was found present at 21 days after injury and had subsided at 119 days after injury. Many GFAP/pS6 immunoreactive cells were found in the dorsal column (Figure 3A, Supporting Information Figure S3A). Few NG2/pS6-immunoreactive cells were found in the ventrolateral white matter (Figure 3B, Supporting Information Figure S3B). Many OX-42/pS6-immunoreactive cells of both round and spiny morphologies were found throughout white matter, with higher concentrations in the dorsal columns (Figure 3C, Supporting Information Figure S3C). A lower concentration of ED1/pS6-immunoreactive cells compared with OX-42/pS6 immunoreactive cells was found throughout white matter (Figure 3D, Supporting Information Figure S3D).

Microglia/macrophages as predominant source of increased S6 phosphorylation

Microglia and macrophages were the predominant pS6-immunoreactive cell population during both identified periods of increased pS6 immunoreactivity after injury. At day 1 post-injury, a higher number of ED-1-immunoreactive activated microglia/macrophages than OX-42 immunoreactive microglia colocalized with pS6 in direct proximity to or within the injury site (Figure 4).

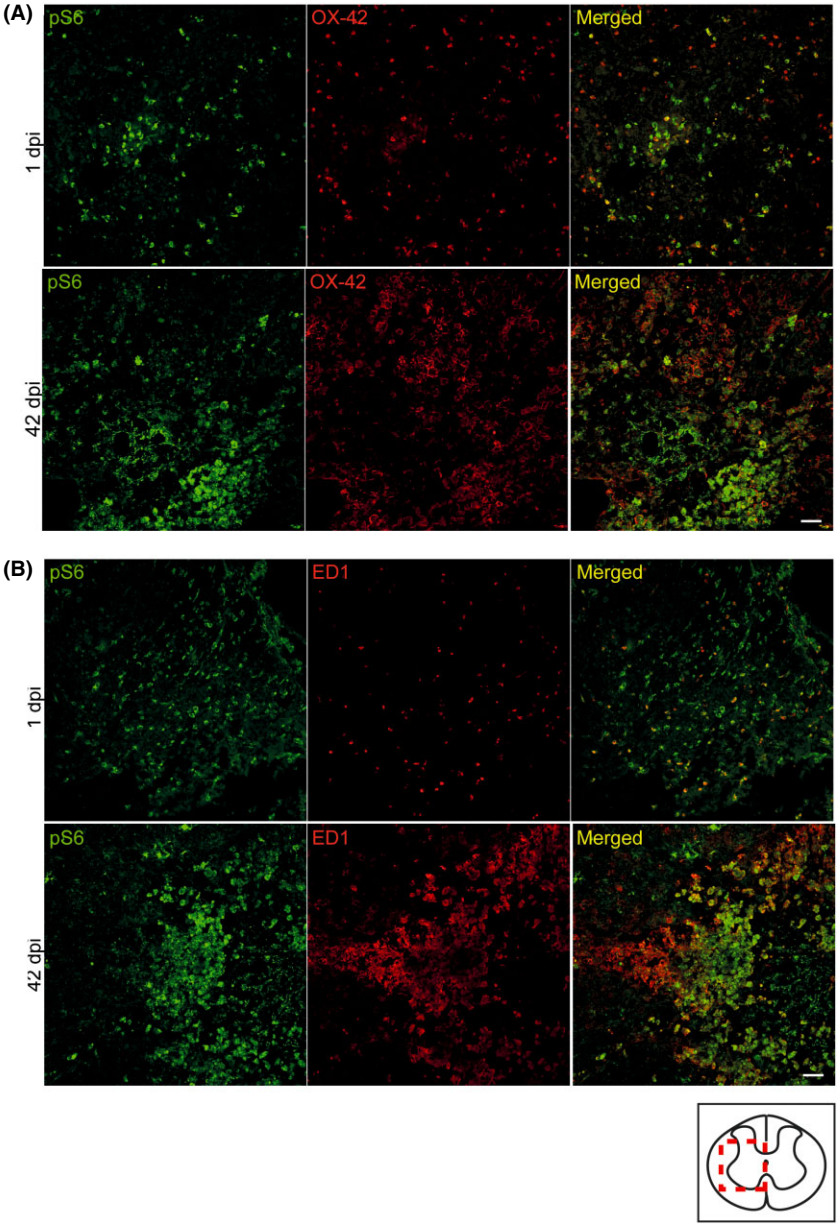

Figure 4. *S6 phosphorylation in many inflammatory cells at the injury site.* Representative pictures from 1 and 42 days after injury at the injury site. **A.** Microglia visualized by OX-42. **B.** Activated microglia/macrophages visualized by ED1. Scale bar = 20 μm.

The opposite was true in white matter rostral and caudal to the injury, in which a larger number of OX-42-immunoreactive microglia displayed pS6 immunoreactivity (Supporting Information Figure S3). Neutrophils, identified by MPO immunoreactivity, did not display pS6 immunoreactivity (Supporting Information Figure S4). Between 21 and 119 days post-injury, we found a similar pattern, although pS6/ED-1-immunoreactive microglia/macrophages constituted the major pS6-positive population at the site of injury (Figure 4). pS6 immunoreactivity was also observed to be higher in spinal cords in which cystic cavities had been formed in the dorsal column caudal to injury, compared with those were none had formed (Figure 5). In the dorsal column rostral to injury, cysts are less common, and this region is instead characterized by increased inflammatory activity. Here we found robust increase of S6 immunoreactivity already after 1 day, the average fluorescence intensity being 5.63 (SEM 0.41) vs. 0.26 (SEM 0.05) in control tissue ($P < 0.001$) (Figure 6). Seven days after injury, we observe a dramatic reduction to almost control levels, followed by a second progressive increase ($P < 0.05$ at 21 days), peaking at 42 days (1.92 ± 0.11, $P < 0.001$). After 17 weeks pS6 immunoreactivity had again returned to levels comparable with those seen in uninjured animals. A similar pattern was found below the site of injury, though less pronounced (Supporting Information Figure S5).

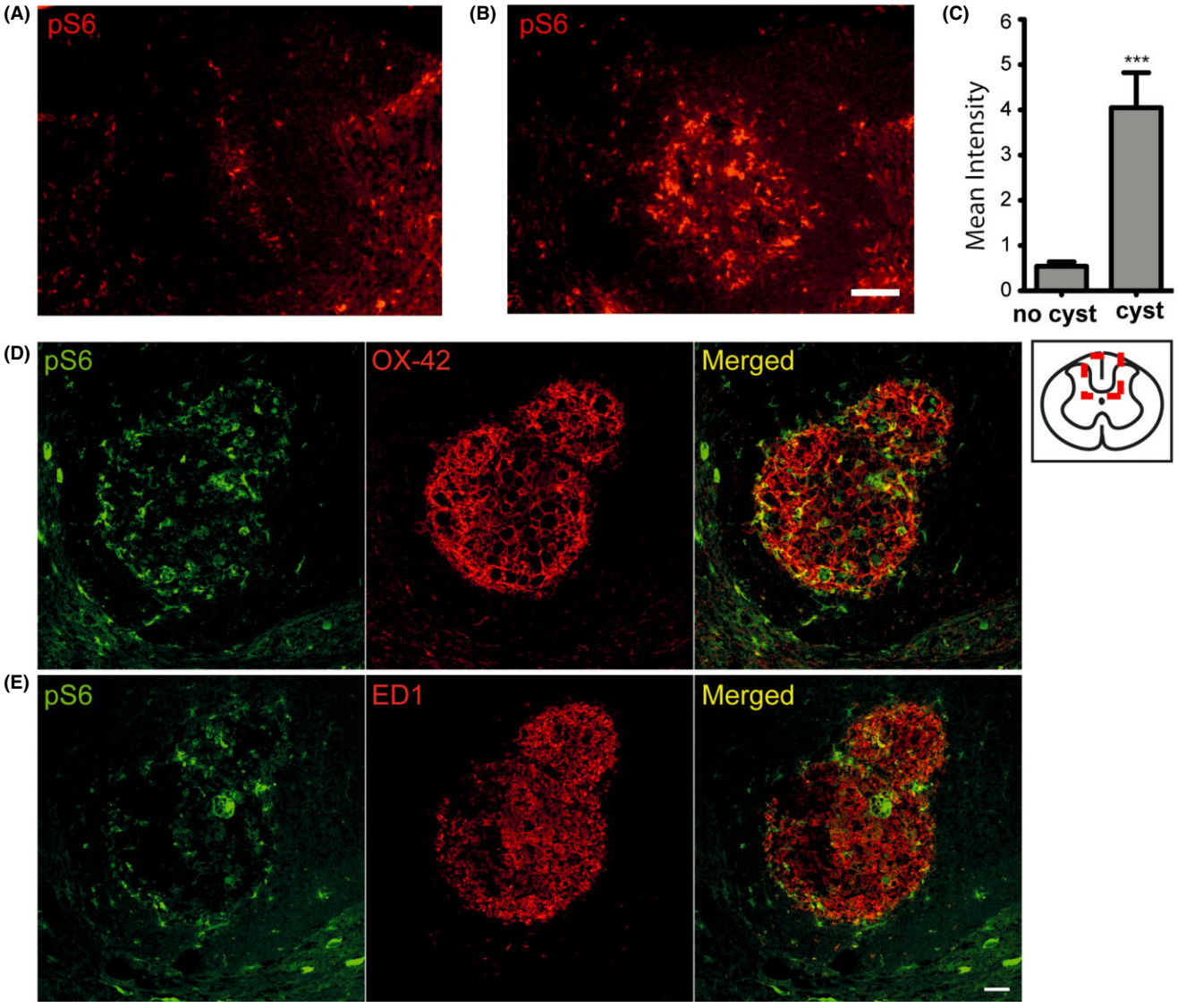

Figure 5. *pS6-positive immune cells within cystic cavities.* Cystic cavities are sometimes formed at the site of the dorsal column caudal to the injury site. **A.** Representative picture of dorsal column at 21 days after injury without cyst (7 mm rostral to injury site). **B.** Representative picture of dorsal column at 21 days after injury with cyst (7 mm caudal to injury site). Scale bar = 50 μm. **C.** Quantification of pS6 immunoreactivity at 21 days after injury without or with a cyst 7 mm caudal to the injury site. **D.** Representative picture of colocalization of pS6 and OX-42 immunoreactivity in the cyst. **E.** Representative picture of colocalization of pS6 and ED1 immunoreactivity in the cyst. Scale bar = 20 μm. Data presented as mean ± SEM. $***P < 0.001$.

Early S6 phosphorylation in proliferating cells

Injury to the cord initiates proliferation of glial cells, and proliferation is a function associated with mTORC1 and S6 activation. At day 1 post-injury, cell proliferation was observed primarily within the ventrolateral white matter and the dorsal column, but also in gray matter. The majority of proliferating cells were pS6-immunoreactive except for those surrounding the central canal (Figure 7, Supporting Information Figure S6). From 7 days onward, few proliferating cells were found, and only single proliferating cells could be found to be pS6-positive during these later time points (Supporting Information Figure S7).

DISCUSSION

Here, we characterize mTORC1 activation after contusion spinal cord injury in rats (Table 1). We used phosphorylation of the ribosomal protein S6 as a readout for mTORC1 activation, as it has been found responsive to mTORC1 inhibition using immunohistochemistry (7). We found that mTORC1 is constitutively active in neurons of the ventral horns and a subpopulation of neurons in the intermediate zone, with little activity seen in glial cells in the uninjured spinal cord. We observed that injury induced a biphasic decrease of mTORC1 activation in neuronal populations rostral and caudal to injury as well as a biphasic increase of mTORC1

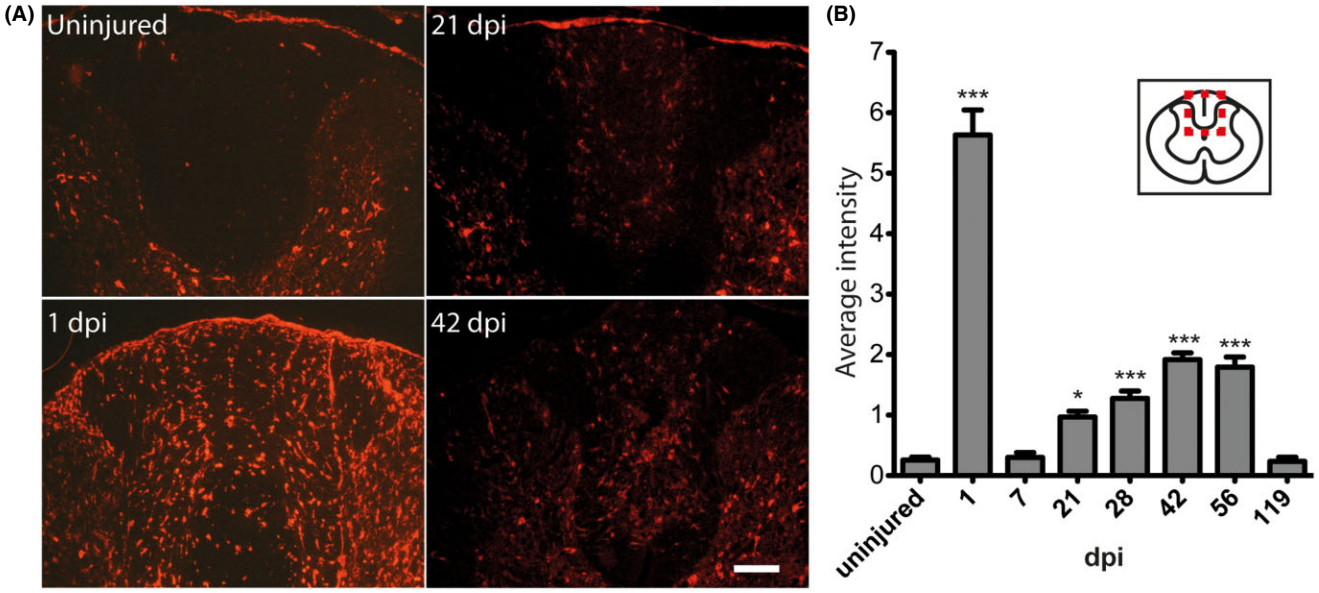

Figure 6. *pS6 immunoreactivity in the dorsal column rostral to the injury site.* **A.** Representative pictures of pS6 immunoreactivity in the dorsal column 7 mm above the injury site in the intact spinal cord and 1, 21, and, 42 days after injury. Scale bar = 50 μm. **B.** Quantification of pS6 immunoreactivity. Data presented as mean ± SEM. $*P < 0.05$; $**P < 0.01$; $***P < 0.001$.

activation in non-neuronal cells that was spatially oriented to regions of the spinal cord with the largest amount of pathology. Characterization of the glial cells with mTORC1 activity revealed that macrophages/microglia and astrocytes were the predominant populations. We also observed that proliferating cells constituted another significant population of cells with injury-induced increase of mTORC1 activity.

To date, studies of mTORC1 activity in spinal cord injury have focused on neurons and astrocytes (6, 26, 34). Certain neuronal populations have previously been shown to have constitutive mTORC1 activation in CNS, and increasing activity in spinal cord injury models has improved neural sprouting (9, 19, 22, 25). Instead, decreasing mTORC1 activity in neurons has been reported to induce autophagy, which is thought to help neurons survive traumatic insults (34). However, prolonged autophagy may induce apoptosis and could be a reason for the observed loss of mTORC1 activity in neurons (8, 15).

Astrocyte reactivity has been shown to decrease with mTORC1 inhibition. However, in our injury model astrocytes remained a small population, as did oligodendrocyte progenitor cells. These glial cells and microglia are known to proliferate during the first days after injury, and we found such proliferating glia to coexpress with phosphorylated S6, known to regulate cell cycle progression (21, 38, 40).

Unexpectedly, we identified microglia/macrophages to be the largest population responsible for the biphasic increases in mTORC1 activity. The first part of the biphasic increase is derived from microglia inherent to white matter, while the second part originates from activated microglia/macrophages, mostly localized to the injury site where there has been infiltration of macrophages from the circulation (3, 29). Activated microglia and macrophages are known to change cytokine expression profiles, activation state, and polarization according to level of mTORC1 activity (5, 20, 23, 32). Identifying biphasic mTORC1 activation in microglia/macrophages provide a possible opportunity to counter the endogenous mTORC1 activity and its effects on microglia/macrophages in the pathophysiology of spinal cord injury. Hence, this finding warrants further research into the function of mTORC1 in microglia/macrophages in spinal cord injury.

Immune cells are known to play a pivotal role in the progressive tissue destruction seen in spinal cord injury, but may also facilitate regeneration in spinal cord injury (10, 16). mTORC1 activation

Table 1. Localization of pS6 immunoreactivity in different immunohistochemically defined cell types. Number of plus signs denotes proportion of pS6 colocalization (a ( ) around the + denotes half a plus). GFAP = glial fibrillary acidic protein; NG2 = neuron-glial antigen 2; MPO = myeloperoxidase.

Days post-injury	Dorsal column	Ventrolateral white matter	Gray matter	Injury site
1				
GFAP	+	+	+	+
OX-42	+(+)	++	++	+(+)
ED1	+	–	+	++
NG2	(+)	(+)	(+)	–
MPO	–	–	–	–
Ki-67	+(+)	++	+	+
42				
GFAP	+	+	++	–
OX-42	+	+	+	++(+)
ED1	(+)	(+)	(+)	+++
NG2	(+)	+	(+)	–
Ki-67	–	–	+	–

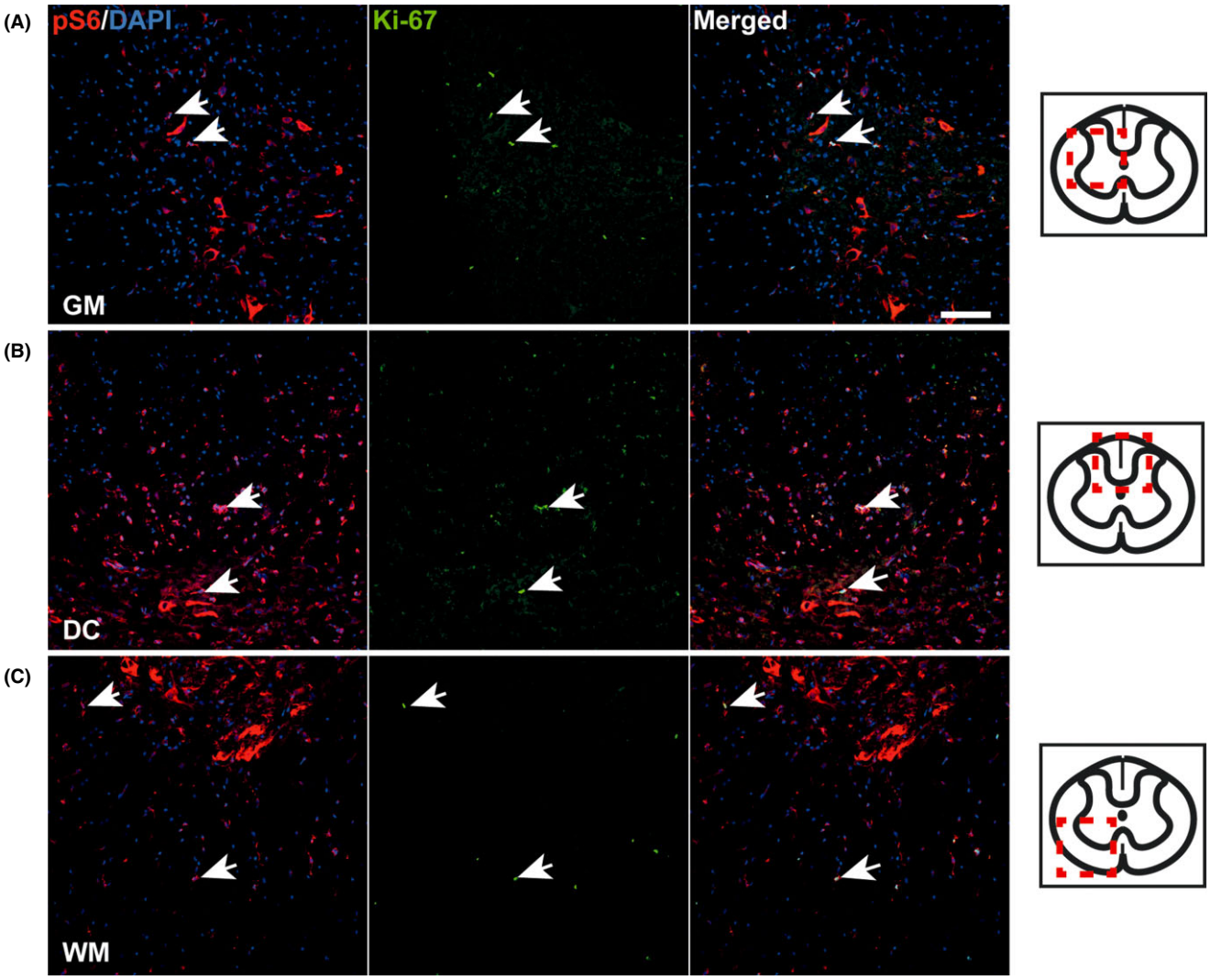

Figure 7. *Proliferating cells pS6-positive at 1 day after injury*. Representative pictures of pS6 and Ki-67 colocalization 1 day after injury 7 mm above the injury site in (**A**) gray matter (GM), (**B**) dorsal column (DC), and (**C**) ventrolateral white matter (WM). Scale bar = 20 μm.

has been associated with driving macrophage populations to become M2 macrophages, a more pro-regenerative state that allows resolution (5). Instead, mTORC1 inhibition may polarize macrophages toward what is known as M1 type, a pro-inflammatory and neurotoxic state causing, for example, increased production of reactive oxygen species (23). Thus, early inhibition might be beneficial, as observed by Sekiguchi *et al* (34), by promoting infiltration of debris-removing macrophages. Instead, late increase of activation may promote resolution and nerve growth as shown, for example, by Liu *et al* (19), and might perhaps reverse the loss of mTORC1 activation we find in neurons bellow the injury. It is also interesting to note that axon regeneration can be synergistically promoted by convergent neuro-immune ligand signaling, and that several of these ligands share the mTOR signaling pathway (11).

The spatiotemporal characterization of mTORC1 activation provided here depicts mTORC1 activation in a pathological context and identifies microglia/macrophages as the major contributors to the biphasic increase after injury. While further research into the function of mTORC1 activation and its significance in spinal cord injury is needed, our findings suggest new windows of opportunity for advancing mTORC1 as a possible target for clinical application.

ACKNOWLEDGMENTS

We thank Professor Lars Olson for constructive review of the manuscript and Karin Pernold for assistance with spinal cord preparation. This study was supported by grants from the Swedish Brain Foundation, the Swedish Research Council, Wings for Life, the Swedish Society for Medical Research (SSMF), the Swedish Agency for Innovation Systems (VINNOVA), and the Karolinska Institutet DPA program.

REFERENCES

1. Abrams MB, Nilsson I, Lewandowski SA, Kjell J, Codeluppi S, Olson L, Eriksson U (2012) Imatinib enhances functional outcome after spinal cord injury. *PLoS One* **7**:e38760.
2. Asante CO, Wallace VC, Dickenson AH (2010) Mammalian target of rapamycin signaling in the spinal cord is required for neuronal plasticity and behavioral hypersensitivity associated with neuropathy in the rat. *J Pain* **11**:1356–1367.
3. Beck KD, Nguyen HX, Galvan MD, Salazar DL, Woodruff TM, Anderson AJ (2010) Quantitative analysis of cellular inflammation after traumatic spinal cord injury: evidence for a multiphasic inflammatory response in the acute to chronic environment. *Brain* **133**:433–447.
4. Caccamo A, Magrì A, Medina DX, Wisely EV, López-Aranda MF, Silva AJ, Oddo S (2012) mTOR regulates tau phosphorylation and degradation: implications for Alzheimer's disease and other tauopathies. *Aging Cell* **12**:370–380.
5. Chen W, Ma T, Shen X-N, Xia X-F, Xu G-D, Bai X-L, Liang T-B (2012) Macrophage-induced tumor angiogenesis is regulated by the TSC2–mTOR pathway. *Cancer Res* **72**:1363–1372.
6. Codeluppi S, Gregory EN, Kjell J, Wigerblad G, Olson L, Svensson CI (2011) Influence of rat substrain and growth conditions on the characteristics of primary cultures of adult rat spinal cord astrocytes. *J Neurosci Methods* **197**:118–127.
7. Codeluppi S, Svensson CI, Hefferan MP, Valencia F, Silldorff MD, Oshiro M *et al* (2009) The Rheb–mTOR pathway is upregulated in reactive astrocytes of the injured spinal cord. *J Neurosci* **29**:1093–1104.
8. Codogno P, Meijer AJ (2005) Autophagy and signaling: their role in cell survival and cell death. *Cell Death Differ* **12**(Suppl. 2):1509–1518.
9. Cota D, Proulx K, Smith KAB, Kozma SC, Thomas G, Woods SC, Seeley RJ (2006) Hypothalamic mTOR signaling regulates food intake. *Science* **312**:927–930.
10. David S, Kroner A (2011) Repertoire of microglial and macrophage responses after spinal cord injury. *Nat Rev Neurosci* **12**:388–399.
11. Gensel JC, Kigerl KA, Mandrekar-Colucci SS, Gaudet AD, Popovich PG (2012) Achieving CNS axon regeneration by manipulating convergent neuro-immune signaling. *Cell Tissue Res* **349**:201–213.
12. Gonzalez R, Glaser J, Liu MT, Lane TE, Keirstead HS (2003) Reducing inflammation decreases secondary degeneration and functional deficit after spinal cord injury. *Exp Neurol* **184**:456–463.
13. Gruner JA (1992) A monitored contusion model of spinal cord injury in the rat. *J Neurotrauma* **9**:123–128.
14. Guerrero AR, Uchida K, Nakajima H, Watanabe S, Nakamura M, Johnson WE, Baba H (2012) Blockade of interleukin-6 signaling inhibits the classic pathway and promotes an alternative pathway of macrophage activation after spinal cord injury in mice. *J Neuroinflammation* **9**:40.
15. Kanno H, Ozawa H, Sekiguchi A, Yamaya S, Itoi E (2011) Induction of autophagy and autophagic cell death in damaged neural tissue after acute spinal cord injury in mice. *Spine* **36**:E1427–E1434.
16. Kigerl KA, Gensel JC, Ankeny DP, Alexander JK, Donnelly DJ, Popovich PG (2009) Identification of two distinct macrophage subsets with divergent effects causing either neurotoxicity or regeneration in the injured mouse spinal cord. *J Neurosci* **29**:13435–13444.
17. Kjell J, Sandor K, Josephson A, Svensson CI, Abrams MB (2013) Rat substrains differ in the magnitude of spontaneous locomotor recovery and in the development of mechanical hypersensitivity after experimental spinal cord injury. *J Neurotrauma* **30**:1805–1811.
18. Laplante M, Sabatini DM (2009) mTOR signaling at a glance. *J Cell Sci* **122**:3589–3594.
19. Liu K, Lu Y, Lee JK, Samara R, Willenberg R, Sears-Kraxberger I *et al* (2010) PTEN deletion enhances the regenerative ability of adult corticospinal neurons. *Nat Neurosci* **13**:1075–1081.
20. Lu D-Y, Liou H-C, Tang C-H, Fu W-M (2006) Hypoxia-induced iNOS expression in microglia is regulated by the PI3-kinase/Akt/mTOR signaling pathway and activation of hypoxia inducible factor-1alpha. *Biochem Pharmacol* **72**:992–1000.
21. Lytle JM, Wrathall JR (2007) Glial cell loss, proliferation and replacement in the contused murine spinal cord. *Eur J Neurosci* **25**:1711–1724.
22. Meikle L, Pollizzi K, Egnor A, Kramvis I, Lane H, Sahin M, Kwiatkowski DJ (2008) Response of a neuronal model of tuberous sclerosis to mammalian target of rapamycin (mTOR) inhibitors: effects on mTORC1 and Akt signaling lead to improved survival and function. *J Neurosci* **28**:5422–5432.
23. Mercalli A, Calavita I, Dugnani E, Citro A, Cantarelli E, Nano R *et al* (2013) Rapamycin unbalances the polarization of human macrophages to M1. *Immunology* **140**:179–190.
24. Morelon E, Mamzer-Bruneel MF, Peraldi MN, Kreis H (2001) Sirolimus: a new promising immunosuppressive drug. Towards a rationale for its use in renal transplantation. *Nephrol Dial Transplant* **16**:18–20.
25. Norsted Gregory E, Codeluppi S, Gregory JA, Steinauer J, Svensson CI (2010) Mammalian target of rapamycin in spinal cord neurons mediates hypersensitivity induced by peripheral inflammation. *Neuroscience* **169**:1392–1402.
26. Pastor MD, García-Yébenes I, Fradejas N, Pérez-Ortiz JM, Mora-Lee S, Tranque P *et al* (2009) mTOR/S6 kinase pathway contributes to astrocyte survival during ischemia. *J Biol Chem* **284**:22067–22078.
27. Pitter KL, Galbán CJ, Galbán S, Tehrani OS, Saeed-Tehrani O, Li F *et al* (2011) Perifosine and CCI 779 co-operate to induce cell death and decrease proliferation in PTEN-intact and PTEN-deficient PDGF-driven murine glioblastoma. *PLoS One* **6**:e14545.
28. Popovich PG, Guan Z, Wei P, Huitinga I, van Rooijen N, Stokes BT (1999) Depletion of hematogenous macrophages promotes partial hindlimb recovery and neuroanatomical repair after experimental spinal cord injury. *Exp Neurol* **158**:351–365.
29. Popovich PG, van Rooijen N, Hickey WF, Preidis G, McGaughy V (2003) Hematogenous macrophages express CD8 and distribute to regions of lesion cavitation after spinal cord injury. *Exp Neurol* **182**:275–287.
30. Popovich PG, Wei P, Stokes BT (1997) Cellular inflammatory response after spinal cord injury in Sprague-Dawley and Lewis rats. *J Comp Neurol* **377**:443–464.
31. Rapalino O, Lazarov-Spiegler O, Agranov E, Velan GJ, Yoles E, Fraidakis M *et al* (1998) Implantation of stimulated homologous macrophages results in partial recovery of paraplegic rats. *Nat Med* **4**:814–821.
32. Russo Dello C, Lisi L, Tringali G, Navarra P (2009) Involvement of mTOR kinase in cytokine-dependent microglial activation and cell proliferation. *Biochem Pharmacol* **78**:1242–1251.
33. Santini E, Heiman M, Greengard P, Valjent E (2009) Inhibition of mTOR signaling in Parkinson's disease prevents L-DOPA-induced dyskinesia. *Sci Signal* **80**:ra36.
34. Sekiguchi A, Kanno H, Ozawa H, Yamaya S, Itoi E (2011) Rapamycin promotes autophagy and reduces neural tissue damage and locomotor impairment after spinal cord injury in mice. *J Neurotrauma* **29**:946–956.
35. Shechter R, London A, Varol C, Raposo C, Cusimano M, Yovel G *et al* (2009) Infiltrating blood-derived macrophages are vital cells

playing an anti-inflammatory role in recovery from spinal cord injury in mice. *PLoS Med* **6**:e1000113.
36. Stallone G, Schena A, Infante B, Di Paolo S, Loverre A, Maggio G *et al* (2005) Sirolimus for Kaposi's sarcoma in renal-transplant recipients. *N Engl J Med* **352**:1317–1323.
37. Villanueva EC, Münzberg H, Cota D, Leshan RL, Kopp K, Ishida-Takahashi R *et al* (2009) Complex regulation of mammalian target of rapamycin complex 1 in the basomedial hypothalamus by leptin and nutritional status. *Endocrinology* **150**:4541–4551.
38. Volarević S, Stewart M, Ledermann B, Zilberman F (2000) Proliferation, but not growth, blocked by conditional deletion of 40S ribosomal protein S6. *Science* **288**:2045–2047.
39. Yilmaz ÖH, Katajisto P, Lamming DW, Gültekin Y, Bauer-Rowe KE, Sengupta S *et al* (2012) mTORC1 in the Paneth cell niche couples intestinal stem-cell function to calorie intake. *Nature* **486**:490–495.
40. Zai LJ, Wrathall JR (2005) Cell proliferation and replacement following contusive spinal cord injury. *Glia* **50**:247–257.

SUPPORTING INFORMATION

Additional Supporting Information may be found in the online version of this article at the publisher's web-site:

Figure S1. Constitutive S6 phosphorylation in neurons in the ventral horns, but not in the dorsal horns. Representative pictures 7 mm rostrally from the injury site of dorsal horn at 1 and 21 days post-injury (**A**), ventral horn at 1 and 42 days post-injury (**B**). Scale bar = 20 μm.

Figure S2. Above injury, the number of pS6 positive neurons returns to basal levels. pS6 and NeuN were used to detect S6 phoshorylation in neurons 7 mm above the injury site. **A.** Representative pictures showing intact tissue and tissue 1, 21, and 42 days after injury. Scale bar = 50 μm. **B.** Quantification of number of pS6- and NeuN-positive cells for all experimental time points. Data presented as mean ± SEM. $*P < 0.05$; $**P < 0.01$; $***P < 0.001$.

Figure S3. Microglia show the greatest proportion of S6 phosphorylation among glial cells in the white matter. Representative pictures of ventrolateral white matter 7 mm rostral to the injury site at 1 and 21 days post-injury showing markers for astrocytes (**A**), oligodendrocyte progenitor cells (**B**), microglia (**C**), activated microglia/macrophages (**D**). Scale bar = 20 μm.

Figure S4. No S6 phosphorylation in neutrophils. Representative picture 1 day after injury at the injury site. Scale bar = 20 μm.

Figure S5. pS6 immunoreactivity in the dorsal column caudal to the injury site. S6 phosphorylation is biphasic in the dorsal column. **A.** Representative pictures of pS6 immunoreactivity in the dorsal column 7 mm below the injury site in the intact spinal cord and 1, 2, and 42 days after injury. Scale bar = 50 μm. **B.** Quantification of time course of pS6 immunoreactivity. Data presented as mean ± SEM. $*P < 0.05$; $** P < 0.01$; $*** P < 0.001$.

Figure S6. No S6 phosphorylation in proliferating cells at the central canal. Representative picture 1 day after injury of the central canal 7 mm rostral to the injury. Scale bar = 5 μm.

Figure S7. Infrequent S6 phosphorylation in proliferating cells 6 weeks after injury. Representative pictures of pS6 and Ki-67 colocalization 7 mm above the injury site in gray matter (GM) (**A**), dorsal column (DC) (**B**), ventrolateral white matter (WM) (**C**). Scale bar = 20 μm.

Figure S8. Fewer NeuN-immunoreactive cell bodies below the injury. Representative pictures from the gray matter 7 mm caudal to the injury site. The dashed line defines the area close to the dorsal column where most of the difference in number of NeuN-positive cells was found. **A**. Uninjured. **B.** 119 days post-injury. **C.** Quantification of number of NeuN-positive cells 7 mm rostral to the injury site. Data presented as mean ± SEM. $***P < 0.001$. Scale bar = 25 um.